Translation Effects on Simulated Tornadoes

CHRIS J. DIAMOND AND EUGENE M. WILKINS[1]

University of Oklahoma, Norman, OK 73019

(Manuscript received 2 February 1984, in final form 5 July 1984)

ABSTRACT

A simulation of tornadoes translating over the ground was carried out in a modified Ward simulator. The purpose was to investigate the effects of translation on tornado dynamics. The results are as follows:

- Secondary vortexes were found to be generated by the relative motion between the main vortex and rough "ground." The secondary vortexes trail the primary vortex. Apparently they feed off the energy of the primary vortex, and achieve a momentary transition state from a single vortex to multiple vortexes.
- The core radius increases with swirl ratio and decreases with surface roughness. Translation causes a local increase in swirl ratio, increasing the core size over that of a stationary vortex.
- The central pressure drop increases with swirl ratio during translation. Translation also causes a steeper pressure gradient on the trailing side of the vortex core. A similar characteristic tilt on the trailing side of the pressure profile has been noted on barograms for real tornadoes.

1. Introduction

The movement of a vortex over the ground must have important effects on its structure and dynamics, but these effects have not been subjected to much, if any, investigation. Two obvious influences (there may be others) are 1) the differential friction velocity on either side of the advancing vortex, and 2) the relative motion, if any, between the vortex and the imbedding air mass. Motion relative to either the ground or the air mass will result in asymmetrical inflow.

The tornado simulator imposes the constraint that the vortex must remain stationary, so we are only able to simulate the relative motion effect by translating the floor beneath the vortex. This is comparable to the situation in which the vortex simply drifts with the air mass.

If important dynamical effects do result from translation, then these need to be identified since the usual laboratory and numerical simulations of tornadoes do not include such effects.

2. Tornado simulator

The tornado simulator used in these experiments is a modified version of Ward's (1972) simulator, a schematic of which is shown in Fig. 1. A fine-mesh screen rotating at a radius of $r_s = 1.22$ m controls the inflow angle θ, measured near the screen (radius r_s) by a small wind vane. Updraft is provided by a variable speed exhaust fan above the convection chamber. Other controlled variables are updraft radius r_0, inflow layer depth h and translation speed v_t.

For these experiments the aspect ratio was set at $a = h/r_0 = 1.2$, with $h = 0.508$ m and $r_0 = 0.457$ m. This ratio favors a stable single vortex with little tendency to wander off center. The vertical profile of inflow velocity was shaped by taping part of the screen. For these experiments $\alpha = \frac{1}{3}$, where α is the exponent for the power-law variation of velocity with height.

The Ward simulator was modified by installing a movable "ground" plate which could be propelled across the floor of the simulator by means of a specifically designed motor drive. The surface of the ground plate was covered with finely crushed rock, as was the floor of the simulator. The transporting mechanism is detailed in Fig. 2. The track was offset so that the pressure port could traverse the center of the simulator. A preset speed was maintained as the plate crossed the convection zone. The speed was monitored on a recorder. A sample graph of speed, acceleration and displacement has been shown by Light (1980).

The ground plate was made as large as practicable in order to minimize edge effects. Its width, 0.45 m, is about five times larger than the diameter of the vortex core, and the length is seven times larger. The length is greater than the radius of the convection zone.

An extremely rough surface was used in order to maximize any response to translation. A roughness length of $z_0 = 0.0034$ m was estimated by means of the Lettau (1969) formula. A scaling factor of approximately 1,000:1 is appropriate for the simulator, so that the corresponding roughness length in the real world would be about 3.4 m. This is four times the

[1] *Also at E-Systems, Inc., Dallas, TX 75266.*

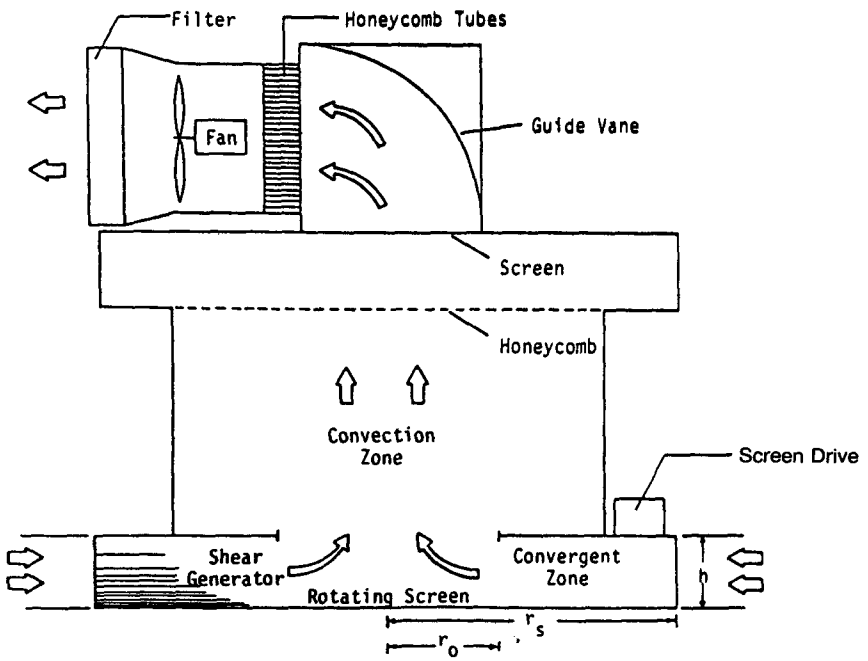

FIG. 1. Schematic of tornado simulator as modified for control of inflow velocity profile.

roughness length used by Leslie (1977) for a simulation of surface roughness effects on multiple vortex transitions.

For realistic simulation of tornadoes we utilize nondimensional scaling parameters which have a magnitude in the simulator well within the range of values believed to occur in nature. The appropriate set of geometric and dynamic scaling numbers (swirl ratio S, Reynolds number Re, aspect ratio a, etc.) has been discussed by Davies-Jones (1973). This same set has been utilized by numerous investigators. These are defined as $S = \tan(\theta)/2a$, $a = h/r_0$, and $\mathrm{Re} = Q/\nu h$, where Q is the flow rate of the simulator and ν is kinematic viscosity.

The practical ranges of the variable parameters for the configuration described above are Re = 20 080 to 40 565, S = 0.096 to 0.554, v_t = 0.308 to 0.768 m s^{-1}: these ranges were used in the experiments. If the laboratory vortex maximum velocity is scaled to an 89 m s^{-1} tornado, then our translation speeds would scale between 6.2 and 15.6 m s^{-1} in the real world.

Pressure profiles constitute the bulk of the quantitative data in this investigation. Pressures are nondimensionalized with respect to air density ρ and radial velocity u_s measured at $r = r_s$, giving $\Delta p/(\frac{1}{2}\rho u_s^2)$ for departures from ambient. In practice, u_s is measured at a height of 13 cm above the floor of the simulator, as we found from experience that this velocity is representative of the flow through the simulator.

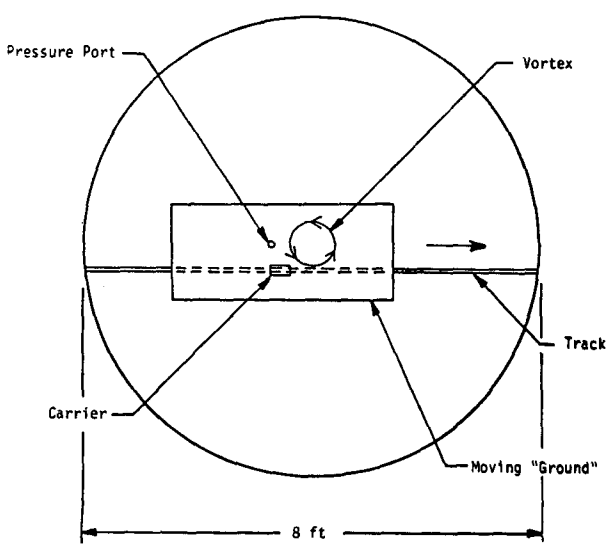

FIG. 2. Schematic of translating surface mechanism.

3. Experimental procedure

The technique depends somewhat on a comparison of vortex properties for stationary and translating conditions. Properties compared include measured pressure profile shape, total pressure drop and vortex diameter.

A sensitive electronic microbarograph recorded the pressure profiles. Every effort was made to eliminate noise due to translation, and especially that due to motion of the pressure tubing, but still it was necessary to prepare repeatable "noise only" traces which subsequently were subtracted from the data runs.

Preparation for a run consisted of generating a single "tornado" in the simulator at a predetermined Reynolds number and swirl ratio. The "ground" plate was then translated beneath the vortex while recording the pressure response and translation speed.

4. Secondary vortexes

Figure 3 is an example of one of the pressure traces, generated as the pressure port moved from left to right (relative motion of vortex is from right to left). A pressure profile for a nontranslating vortex is included for comparison. The difference in swirl ratio for the two cases is unimportant for our purpose, since over the extremely rough surface neither vortex is near the critical value for transition or breakdown. Experiments by Leslie (1977) and Light (1980) verify that the difference in Re is negligible. Light (1980) provides the only case available for making a comparison of this kind. Note that a small secondary vortex appears to trail the "moving" main vortex at a distance of $0.5r_s$, or about 0.61 m (a scaled distance of 0.61 km). This occurred on 19 of the 20 runs that were made successfully. In five cases two or more trailing vortexes were in evidence. Figure 4 is a perspective drawing to show the most frequent location of the secondary vortex when encountered by the pressure probe. Although flow visualization was very difficult, we were able to verify, using a smoke tracer, that one or more secondary swirls actually do occur behind the main vortex. It was not possible to infer the sense of circulation. The secondary vortexes are nonsteady and appear to rapidly combine with the main vortex after translation.

Apparently the secondary vortexes are generated by the interaction between the main vortex and the moving plate. Although we have not identified all of the relevant factors of this interaction, we believe

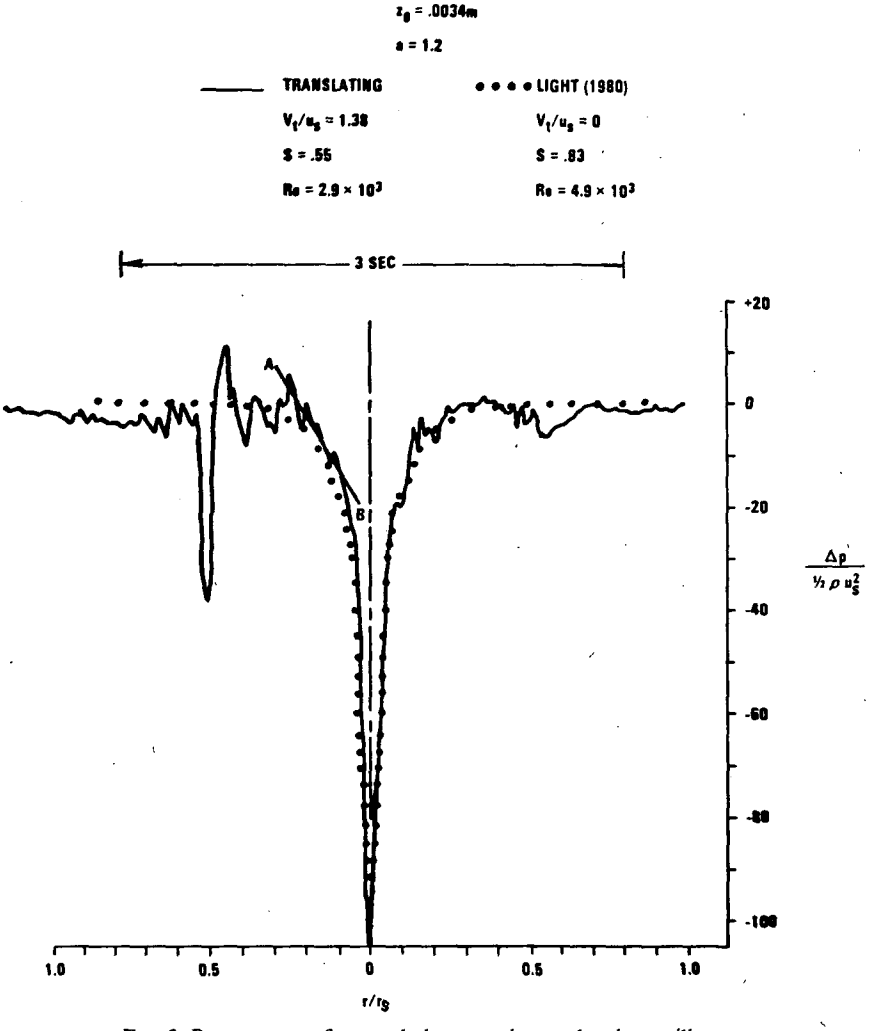

FIG. 3. Pressure trace for translation experiment showing trailing vortex. Pressure profile for a stationary vortex is superimposed for comparison.

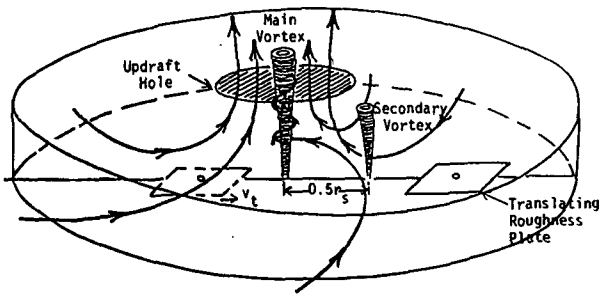

FIG. 4. Schematic showing usual place where secondary vortex is encountered by the pressure probe, which is 15 cm beyond the updraft hole of radius 45.7 cm.

that these secondary vortexes may be related to some types that are observed in nature. Williams (1967) describes graphically his observations of secondary dust whirls. One of the dust whirl episodes reported by Jordan (1980) yielded pressure profiles which are logically explained as a trailing vortex situation. Trailing vortexes have also been observed in tornado and waterspout occurrences.

Williams (1967) gives a sketch from which an estimate of 60 m can be made for the spacing between a primary and trailing secondary vortex. This is a simulator scale factor of 50, which is about right for whirlwinds. Numerous tornado incidents, notably those connected with the Palm Sunday outbreak in 1965, could possibly be related to our experimentally observed transition phenomenon. Fujita (1976) has identified four such classifications: orbiting, peripheral, stray and fringe vortexes. He derived these from multiple vortex situations such as occurred with the Palm Sunday outbreak, and these classifications suggest that there may be more than one mechanism. Also incidences such as that of the Wamego, Kansas, tornado of 15 May 1943, show similarities to that found in our experiments (see p. 27, Flora, 1958) where a small tornado is seen in the vicinity of a larger one.

We noted that the main vortex appeared to be weaker the stronger the secondary vortex, leading to the belief that the secondary vortex splits off, taking away energy. Since the total pressure drop in a vortex is equivalent to its potential energy, the sum of their pressure drops should yield an estimate of the total energy that the primary vortex would have had alone. This sum should also correlate better with the swirl ratio than does the primary pressure drop alone. This is the case; the correlation coefficient is 0.84 as opposed to 0.73. Figure 5 is a plot of the sum of maximum pressure drops versus swirl ratio. The scatter in part was due to varying translation speed and other parameters at single values of the swirl ratio. Also, the pressure probe may not always traverse the center of the secondary vortex. In the flow visualization experiments, the secondary vortex appears to spiral back into the main vortex after the "ground" plate stops translating. Presumably the main vortex may then regain the energy lost from splitting.

We considered the possibility that the secondary vortex might be due to an interaction of the leading edge of the translating surface with the inflow boundary layer. Even a horizontal vortex could cause a pressure pulse. However, only vertical vortexes were seen in the flow visualization.

It seems likely that the splitting results from a momentary transition to a multiple vortex situation caused by a local inflow angle asymmetry peculiar to a translating vortex. In a region of swirling flow it is possible that disturbing the symmetry may create a local excess of vorticity and generate a secondary vortex. In the simulator we are able to increase the number of vortexes by increasing the swirl ratio of the whole simulator, but after the first transition, symmetry is destroyed and there are two translating vortexes. Therefore, the theory of transitions to numbers greater than two must account for translation effects. In these experiments we disturbed the symmetry by introducing relative motion with respect to a very rough surface.

5. Effect of surface roughness

Simulator experiments by Dessens (1972) showed that one effect of increasing the surface roughness was to enlarge the core of the vortex. Wilkins *et al.* (1974) numerically simulated a rough surface condi-

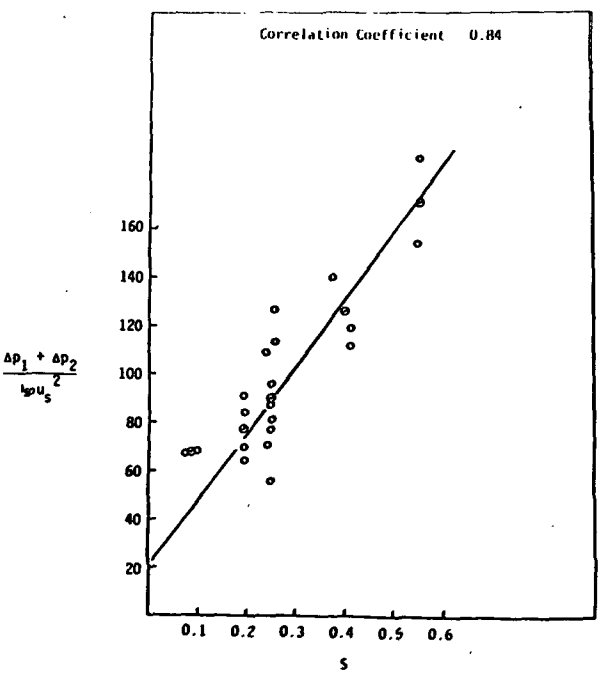

FIG. 5. Sum of primary and secondary maximum pressure drops vs swirl ratio for translating systems. Dots represent group averages.

tion by introducing an Ekman layer. The results tended to verify Dessens' findings. Laboratory simulations of vortex formation by Wilkins *et al.* (1975), using smooth and rough surfaces, yielded excellent agreement with the numerical simulation.

All of these experiments were carried out under high-aspect-ratio conditions. However, Leslie (1979) demonstrated the existence of a critical product of aspect ratio and swirl ratio (aS) at which surface friction has no effect on vortex core size. The hyperbolic curve representing the critical combination is given by $aS = 0.63$ if the Reynolds number, having only a small effect, is neglected. Smaller values of aS represent core size decreasing with surface roughness. In the Ward simulator at the University of Oklahoma, transition from single to double vortex occurs over a smooth surface at $S = 0.23$; so we are constrained to an aspect ratio of 2.74 in the single vortex regime if the core radius is not to change with surface roughness. The largest aspect ratio ever used with the simulator is 1.67, explaining why core radius was always observed to decrease with roughness length. However, the larger aspect ratios may not occur in nature since experimentally, at least, they prohibit multiple vortex transitions. This opinion has also been expressed by Ward (1972) and by Davies-Jones (1973).

Plots of core radius versus swirl ratio are presented in Fig. 6 for Ward simulator experiments over smooth and rough surfaces. A data set by Ward (1972) for a smooth surface, if plotted, would have fallen on Leslie's (1979) data. Data from the translation experiments are included for comparison. Vortex dimensions for the latter group were determined from pressure profiles, whereas the others were measured visually. The two methods are found to yield essentially the same results.

The characteristic increase in core size with swirl ratio is evident in all cases, as is the suppression due to surface roughness. The core radii for the translation experiments (data set 6) unexpectedly are larger than those measured by Light (1980) (data set 2) under otherwise identical circumstances.

In retrospect, we presume that there was a local increase in swirl ratio caused by the translation, giving rise to increased core size. This reasoning is consistent with the observation that a momentary transition to a multiple vortex system occurs during translation. Interestingly, translation has an effect opposite to that of increasing the surface roughness. Blechman's (1974) observations of real tornadoes (supported by experiments of Leslie, 1977) indicate a downward shift in effective swirl ratio due to increased surface roughness.

6. Other pressure profile characteristics

Returning to Fig. 3, we note that the pressure profile is not symmetric about the centerline drawn

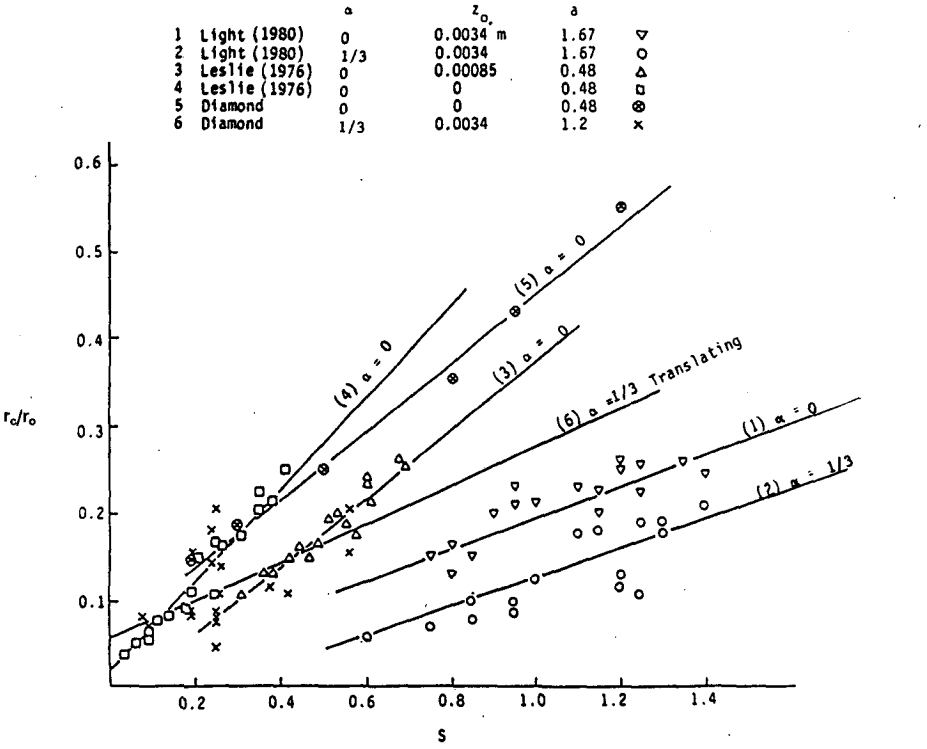

FIG. 6. Core radius vs swirl ratio for stationary and translating vortexes over smooth and rough surfaces.

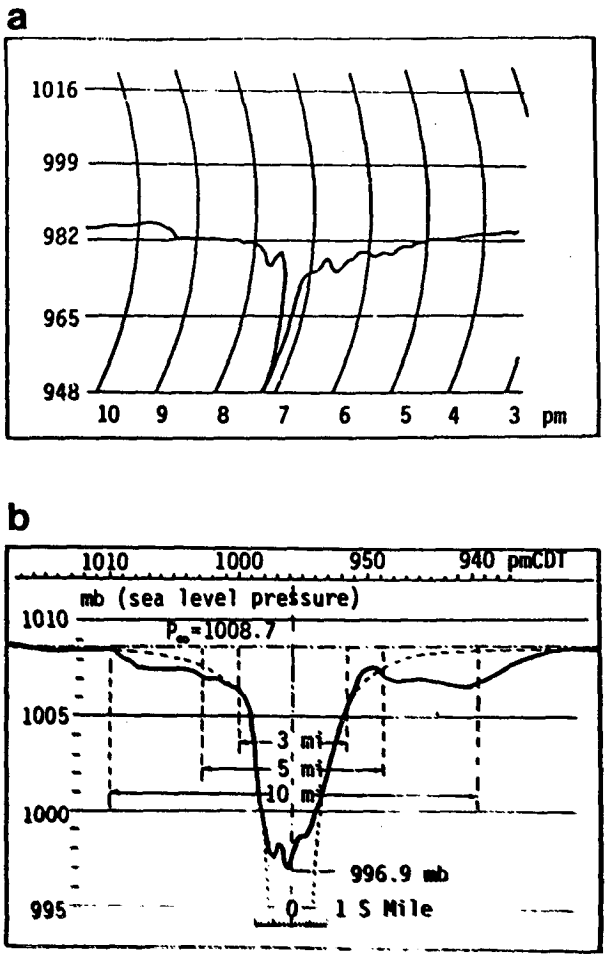

FIG. 7. Examples of tornado proximity pressure traces (a) with the high pressure ring (Ward, 1964) and (b) without (Fujita, 1970).

through the pressure minimum, as was the case for the nontranslation profile of Light (1980). Light's profile was made from a series of static pressure ports, closely spaced along a radial. For the translating case, a region (ring) of relatively higher pressure is evident on the front side of the vortex but is confused on the aft side by the secondary vortex.

a. High pressure ring

Ward (1972) noted that a ring of relatively high pressure occurs about a vortex at low swirl ratio if the aspect ratio is less than about 0.50. As the converging flow approaches the center, the pressure increases as the radial flow decreases, changing into updraft. According to Snow (1982), there is a separation of the inflow from the surface in a ring-like configuration associated with this pressure profile. Reattachment may occur on the inside of the ring.

Ward (1964) also noted that the trailing side of the high pressure ring appeared to be enhanced in the case of the 1962 Newton, Kansas tornado. This asymmetry of the ring is especially pronounced on microbarograms made by Jordan (1980) for passages of whirlwinds. Jordan indicated that his whirls were largely convective (mostly updraft) which places them in the low swirl ratio category, found experimentally to be a requirement for the high pressure ring. We have examined seven other microbarograms for tornado passages, and found that five of these pressure traces show the same upward tilt aft that was pointed out by Ward. The other two did not exhibit a feature identifiable as a high pressure ring; both of these were multiple vortex (high swirl ratio) tornadoes. Figure 7 shows examples of tornado proximity pressure traces with and without the high pressure ring.

In our translation experiments the high pressure ring was usually identifiable at a low swirl ratio, but due to increased pressure noise on the trailing side it was difficult to ascertain that the ring is enhanced there, as is also evident in Fig. 3. However, the pressure gradient just aft the V-shaped (core) region of the profile becomes steeper as the translation speed increases (see line AB in Fig. 3). This is true for all cases, regardless of swirl ratio. The characteristic tilt due to translation is present even when a high pressure ring is not.

Figure 8 is a plot of the nondimensional aft pressure gradient versus nondimensional translation speed. The correlation coefficient is +0.83. No significant correlation was found for the forward pressure slope.

Near the "ground" the translation vector is opposite the radial inflow component on the aft side, and the inflow is therefore diminished relative to the tangential component. This should give an increase in swirl ratio locally. We know experimentally that vortex intensity increases with swirl ratio up to the critical value at which multiple vortex transition occurs. The result of increased tangential velocity should be a local readjustment of the pressure gradient in conformance with the velocity increase.

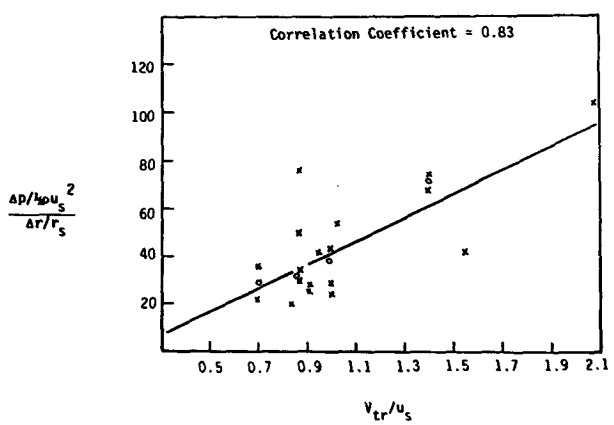

FIG. 8. Aft pressure gradient vs translation speed. Circles represent group averages.

b. Shape factor

We define the shape factor as the ratio of the maximum depth of the pressure trace to its width at the half-depth point. Since all of our traces are V-shaped within the core region, the vortex intensity evidently tends to increase with increasing shape factor. Figure 9 shows the relationship of shape factor to translation speed. The correlation coefficient is +0.645, which is significant, but not overwhelming. The mechanism may be the same as that which causes the aft pressure gradient to increase with increasing translation speed, but we have no evidence to support this.

7. Conclusions

It is possible that trailing vortexes observed in nature have their origin in a mechanism similar to that deduced from our simulator experiments, namely a local swirl ratio increase beyond the transition point. The observed increase in vortex core radius due to translation is consistent with this theory. The logical place for such an enhancement is on the left side of the advancing (cyclonic) vortex. Here, the swirl ratio receives a boost from two sources: the tangential component is augmented by the relative motion between the translation vector and the ground; and the radial component is decreased by reduced frictionally-induced inflow at the ground. By similar reasoning, translation must act to decrease the swirl ratio locally on the right hand side. The extreme roughness of the surface may serve to amplify the process, whereas for a stationary vortex, increased roughness tends to decrease the effective swirl ratio and inhibit transition at this aspect ratio. The difference, then, must be due to the asymmetrical inflow induced by translation.

A search was made for pressure profile characteristics which could help identify tornado dynamical stages and configurations, and also possibly explain translation effects. The most useful features appear to be the tilt of the high pressure ring when it exists, the relationship of aft pressure gradient and shape factor to translation speed, and the vortex enlargement and possible splitting due to translation over a rough surface.

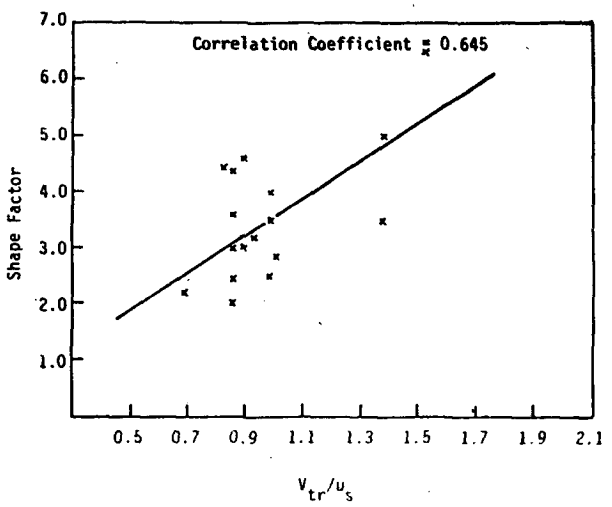

FIG. 9. Shape factor vs translation speed.

Acknowledgments. We are grateful to many people at the University of Oklahoma for assistance with this program. Drs. Robert P. Davies-Jones, Yoshi K. Sasaki, Fred W. Leslie, and especially Dr. A. Sundara-Rajan are thanked for consultations. Mr. Bruce Light, and especially Mr. Fay Moslehi are thanked for assistance with the experimental phase of the program.

The Division of Atmospheric Sciences, National Science Foundation, provided both technical and financial support under Grants ATM 8002102 and ATM 8211399.

REFERENCES

Blechman, J. B., 1974: The Wisconsin tornado event of April 21, 1974: Observations and theory of secondary vortices. *Preprints Ninth Conf. Severe Local Storms,* Norman, OK, Amer. Meteor. Soc., 344–349.

Davies-Jones, R. P., 1973: The dependence of core radius on swirl ratio in a tornado simulator. *J. Atmos. Sci.,* **30,** 1427–1430.

Dessens, J., Jr., 1972: Influence of ground roughness on tornadoes. *J. Appl. Meteor.,* **11,** 72–75.

Flora, S. D., 1958: *Tornadoes of the United States,* 2nd ed. (rev.), University of Oklahoma Press, 221 pp.

Fujita, T., 1970: The Lubbock tornadoes: A study of suction spots. *Weatherwise,* **23,** 161–173.

——, 1976: History of suction vortices. *Proc. Symp. on Tornadoes and Implications for Man,* NUREG/AMS, Texas Tech University, 78–88.

Jordan, A. R., 1980: Pressure and vorticity transients from summer storms and aircraft. *J. Appl. Meteor.,* **19,** 1223–1233.

Leslie, F. W., 1977: Surface roughness effects on suction vortex formation: A laboratory simulation. *J. Atmos. Sci.,* **34,** 1022–1027.

——, 1979: Dynamic behavior of single and multiple vortex tornadoes inferred from laboratory simulation. Ph.D. dissertation, University of Oklahoma, 139 pp.

Lettau, H., 1969: Note on aerodynamic roughness parameter estimation on the basis of roughness element description. *J. Appl. Meteor.,* **8,** 828–832.

Light, B. D., 1980: Laboratory simulation of tornadic wind loads on structures. M.S. thesis, University of Oklahoma, 186 pp.

Snow, J. T., 1982: Pressure fields beneath tornado-like vortices. *Topics in Atmospheric and Oceanographic Sciences,* L. Bengtsson and J. Lighthill, Eds., Springer-Verlag, 259–270.

Ward, N. B., 1964: The Newton, Kansas tornado cyclone of May 24, 1962. *Preprints Eleventh Weather Radar Conference,* Boulder, Amer. Meteor. Soc., 410–415.

——, 1972: The exploration of certain features of tornado dynamics using a laboratory model. *J. Atmos. Sci.,* **29,** 1194–1204.

Wilkins, E. M., Y. K. Sasaki, R. L. Inman and L. L. Terrell, 1974: Vortex formation in a friction layer: A numerical simulation. *Mon. Wea. Rev.,* **102,** 99–114.

——, —— and H. L. Johnson, 1975: Surface friction effects on thermal convection in a rotating fluid: A laboratory simulation. *Mon. Wea. Rev.,* **103,** 305–317.

Williams, N. R., 1967: Whirlwinds. *Encyclopedia of Atmospheric Science and Astrogeology,* Reinhold, 1138–1143.